Research Paper
Computational Methods for Differential Equations
http://cmde.tabrizu.ac.ir
Vol. *, No. *, *, pp. 1-21
DOI:10.22034/cmde.2025.65870.3055

Investigating soliton dynamics for (2+1)-dimensional stochastic Heisenberg ferromagnetic spin-chain model with multiplicative white noise using improved modified extended tanh function technique

Karim K. Ahmed[1], **Hamdy M. Ahmed**[2], **Abeer S. Khalifa**[3], **Mostafa Eslami**[4,*]

[1]Department of Mathematics, Faculty of Engineering, German International University (GIU), New Administrative Capital, Cairo, Egypt.

[2]Department of Physics and Engineering Mathematics, Higher Institute of Engineering, El Shorouk Academy, El Shorouk City, Cairo, Egypt.

[3]Department of Mathematics, Faculty of Basic Sciences, The German University in Cairo (GUC), Cairo, Egypt.

[4]Department of Applied Mathematics, Faculty of Mathematical Sciences, University of Mazandaran, Babolsar, Iran.

Abstract

The stochastic Heisenberg ferromagnetic spin chain equation (SHFSCE) is a fundamental part of modern magnetism theory. The long-range ferromagnetic ordering magnetism with nonlinearity was explained by SHFSCE. It also shows the magnetism of various insulating crystals and interacting spins. Furthermore, ferromagnetism is fundamental to modern industry and technology and serves as the foundation for a number of electrical and electromechanical devices, such as generators, electric motors, and electromagnets. In this work, the nonlinear (2+1)-dimensional HFSCE is effectively solved using the improved modified extended (IME) tanh function technique, and its exact solutions are examined. We therefore give several new precise solutions, such as Jacobi elliptic functions (JEFs), (bright, singular, dark) solitons, rational solutions, singular periodic solutions, Weierstrass elliptic doubly periodic type solutions, and exponential solutions. These new solutions have never been reported before in the models studied. Single solitons that have never been seen before are the novel solutions for the research model. Furthermore, the discovered solutions are used to create a number of fascinating 2D and 3D figures. The geometrical representation of the SHFSCE provides the dynamical information required to describe the physical phenomena. The results are crucial for understanding and studying the (2+1)-dimensional SHFSCE. In order to find distinct soliton solutions and other accurate solutions for various kinds of nonlinear differential equations (NLDEs), more studies on the IME tanh function technique may help. This discovery represents a significant breakthrough in our understanding of the complex and unpredictable behaviour of this mathematical model.

Keywords. SHFSCE, Stochastic solitons, Magnetism theory, NPDEs, IME tanh function algorithm, Analytic method.
2010 Mathematics Subject Classification. 35R60, 35C07, 35C08, 35C09.

1. Introduction

Examining traveling wave solutions for nonlinear evolution equations (NLEEs) is essential for understanding the inner workings of complicated processes. Over the past few decades, significant advancements have been made in the fields of electromagnetism, mechanics of liquids, atomic materials, complex physics, electrical engineering, optical fibers, and geochemistry, among others, and numerous effective and proficient techniques for obtaining analytical traveling wave solutions have been discovered in the literature [1, 2, 4, 11, 16, 20, 48]. As a consequence, a great deal of mathematicians and physicists attempted to devise different techniques to find solutions to these kinds of equations. Soliton theory is important for many nonlinear models when it comes to explaining many intricate events in the field of NLEEs. Soliton dynamics in various models have been researched by many scientists [3, 5, 18, 23, 32, 35, 50]. Systems having unexpected implications are studied using the mathematical technique known as stochastic partial differential equations (SPDEs) [8, 10, 38, 45]. For real or artificially generated complex systems, these kinds of equations can be

Received: 13 February 2025 ; Accepted: 02 September 2025.
∗ Corresponding author. Email: mostafa.eslami@umz.ac.ir.

utilized to simulate a broad range of stochastic dynamics. The basis of SPDE theory is modern stochastic analysis and the study of deterministic partial differential equations. It is possible to derive effective solutions for non-negative partial differential equations, which can aid in the understanding of many physical processes.

The last few years have seen major advancements in the research of NLDEs of water wave models in [24] using Lie symmetry analysis. The generalized (3+1) dimensional cubic quasi-linear Schrödinger equation with certain spatial distribution parameters was solved mathematically precisely by Kumar et al. [22] using space-time periodic traveling wave solutions. Bulut et al. [14] used the potent sine-Gordon expansion approach to look for solutions to several significant nonlinear mathematical models that emerge in nonlinear sciences. The soliton solutions with dual power law nonlinearity and fourth-order dispersion to the nonlinear Schrödinger equation were studied by Zayed et al. [47], and many various investigations were done on different models [6, 19, 33].

One of the most crucial equations in contemporary magnetic theory for explaining the behavior of nonlinear magnets is the (2+1)-dimensional SHFSCE. In the soliton theory, the (2+1)-dimensional SHFSCE is of great importance as a suitable equation describing spin-long ferromagnetic ordered interactions and several insulating magnetic crystal characteristics [49]. Soliton solutions for the (2 + 1)-dimensional SHFSCE are characterized by high-quality and qualitative research for numerous phenomena and applications in a range of domains, such as ferromagnetic materials, nonlinear optics, and optical fibers. Meanwhile, at the classical and semiclassical continuous limits, the Heisenberg model of ferromagnetic spin chains with diverse magnetic interactions connected to NLEEs shows a clean and orderly behavior [46]. Another viable option for triggering spin reversal events in ferromagnets is inhomogeneous exchange interactions [15]. To create accurate traveling wave solutions, the authors of [25] used the modified Kudryashov and another transformation approach called Darboux in 2014. Inc et al.'s [21] approach of using the generalized tanh and complex envelope functions allowed them to resolve the soliton solutions of the Heisenberg ferromagnetic spin chain (HFSC) problem in two dimensions. Ma et al. [30] investigated soliton solutions of the 2D-HFSC problem in 2018 using the Jacobi elliptic approach and an enhanced F-expansion method. Using the Hirota bi-linear approach, Li and Ma [26] selected appropriate polynomial functions in bi-linear forms. As a result, the existence condition and solution for the one-order rogue waves were found. Using the novel extended FAN sub-equation approach, Osman et al. [34] looked into the various wave structures of the 2D-HFSC equation. The authors in [13] utilized the improved F-expansion technique and modified simple equation (MSE) to provide exact solutions for the HFSCE. They used the Jacobi elliptic functions (JEFs) approach to examine the HFSCE in [17]. The HFSCE for the novel accurate solitary solutions was studied by Sahoo and Tripathy [37] using a modified version of Khater's approach. The authors of [49] examined many exact solutions in deterministic form for the (2+1)-dimensional HFSCE, based on Jacobi Elliptic function concepts.

In this work, we investigate the upcoming (2+1)-dimensional SHFSCE which can be read as [17, 34, 49]:

$$i\psi_t + \eta_1\psi_{xx} + \eta_3\psi_{xy} + \eta_2\psi_{yy} - \eta_4\psi|\psi|^2 + \varrho\psi W_t = 0, \tag{1.1}$$

where

$$\eta_1 = \sigma^4(\gamma + \gamma_2), \qquad \eta_2 = \sigma^4(\gamma_1 + \gamma_2), \qquad \eta_3 = 2\sigma^4\gamma_2, \qquad \eta_3 = 2\sigma^4\mathcal{B}. \tag{1.2}$$

In this case, the wave propagation is represented by the complex-valued function $\psi(x, y, t)$, the spatial variables are x and y, and the time variable is t. The anisotropic parameter is designated as $\mathcal{B}$ [17, 34], and the lattice parameter is represented as σ with the interaction coefficients γ, γ_1 and γ_2, and the parameters pertaining to magnetic coupling coefficients are η_i, $1 \le i \le 4$ [27]. Besides, ϱ represents the noise intensity coefficient, whereas one one-dimensional standard form of the Wiener process is represented by $W(t)$. The last term of (1.1) includes the white noise, which is represented by W_t. The following characteristics of the Wiener process are listed in [7, 9, 12, 31, 36, 51]:

(i): $W(t)$ has trajectories that are continuous for $t \ge 0$.
(ii): There are independent increments for $s < t$ in $W(t) - W(s)$.
(iii): The distribution of $W(t) - W(s)$ is normal, with variance $= t - s$ and mean $= 0$.

Thus, the search for soliton solutions in the aforementioned SHFSC model in (1.1) serves as our primary source of inspiration. We want to do this by utilising the IME tanh function algorithm, a freshly developed and trustworthy technique. The approach has the potential to resolve unresolved issues from earlier research. The main objective of the IME tanh function algorithm is to find analytical solutions for a specific generalized stochastic nonlinear Schrödinger

problem. The fundamental objective is to simplify the equation while preserving its key aspects. Standardization makes it easier to find exact solutions and offers crucial details about the behaviour of the system that the SPDE defines.

This work's analytical methodology is based on symbolic computation, which necessitates substantial algebraic operations that are frequently performed using computer algebra programs like Mathematica or Maple. Symbolic approaches might require intricate and time-consuming computations, but they are effective for obtaining precise closed-form solutions. The variational method, Hamiltonian-based methods, and Wang's direct mapping method [28, 29, 43, 44], on the other hand, provide straightforward and simplified frameworks that can lessen the computing load and expedite the solution process, but all these methods don't provide a wide range of exact solution like the method implemented in this paper. These non-symbolic techniques have been effectively used to derive soliton and wave structures with little algebraic overhead, and they are especially useful for specific classes of nonlinear evolution equations. Talking about these techniques not only puts the selected strategy in context but it also identifies possible avenues for further research that prioritize computing efficiency [39–42].

1.1. **Motivation of this study.** In spintronic systems, where thermal noise and quantum fluctuations are important, the SHFSCE is essential for simulating magnetization dynamics. Its stochastic character mimics the actual conditions seen in magnetic materials at the nanoscale. Designing reliable spin-based devices requires an understanding of noise-driven spin wave propagation and stability, which may be gained by studying exact solutions of this model. This serves as the driving force for the analytical investigation conducted in this paper.

1.2. **More physical background about Eq. (1.1).** The SHFSCE represents the interaction of deterministic spin-precession driven by exchange interactions and random fluctuations caused by the environment. This approach is essential for studying magnetization dynamics under non-equilibrium situations, such as noise-induced switching, stochastic resonance, and the suppression or amplification of spin wave propagation. Furthermore, it provides a theoretical framework for investigating stability qualities, coherence loss, and localization phenomena in spin chains subjected to thermal noise effects, which are critical to the operation of spintronic memory and logic components at the nanoscale. Thus, analytical investigations of this equation, particularly those providing precise or soliton-like solutions, are critical for understanding and managing noise-driven spin dynamics in modern magnetic systems.

The following is the structure of our article: Section 1 delivers an overview of the proposed model along with an explanation of its theory. Given in Section 2, these are the prominent features of the IME tanh function algorithm. In Section 3, all of the results are summarised using Wolfram Mathematica software, which does a thorough symbolic calculation to get these few classes of accurate solutions. The dynamic wave patterns of numerous different soliton solutions are visually shown in Section 4 using both 2D and 3D simulations. In Section 5, we present some discussion about the obtained results. Section 6 presents the conclusions of the work.

2. Preliminaries of the IME tanh function algorithm

The IME tanh function algorithm is a helpful tool for PDE solutions. It can solve complex boundary conditions and offers accurate and efficient solutions for both linear and nonlinear equations. It also provides easily understood and implementable answers. It provides an understandable physical explanation of the solutions, which helps to explain the underlying phenomena. In this section, we outline the key elements of the IME tanh function algorithm that will be used in this research. Consider the succeeding NLPDE [1, 2]:

$$\mathcal{P}\left(\mho, \mho_t, \mho_x, \mho_y, \mho_{xx}, \mho_{tt}, \mho_{xt}, \mho_{xy}, \ldots\right) = 0, \tag{2.1}$$

here $\mathcal{P}$ denotes a polynomial function with its argument $\mho(x, y, t)$ accompanied to its respective partial derivatives.
Step (I): Here, our goal is to change Eq. (2.2), an NLPDE, into a non-linear ordinary differential equation (NLODE). To do this, we use the following transformation:

$$\mho(x, y, t) = \mathcal{V}(\zeta) e^{i(\kappa x + \mathfrak{l} y - ct)}, \qquad \zeta = \mathbf{a}x + \mathbf{b}y - \omega t, \tag{2.2}$$

here $\mathcal{V}(\zeta)$ denotes the amplitude component of the solution, and κ, $\mathfrak{l}$, c, $\mathbf{a}$, $\mathbf{b}$ and ω are defined as real constants which shall be calculated lately in the progress of the work.

Next, we combine Eq. (2.2) with Eq. (2.1), allowing us to build the necessary NLODE as follows:

$$\mathcal{S}(\mathcal{V},\ \mathcal{V}',\ \mathcal{V}'',\ \mathcal{V}''',\ \ldots) = 0, \qquad ' = \frac{d}{d\zeta}. \tag{2.3}$$

Step (II): According to the used algorithm, the general form of the solution for Eq. (2.3) is as follows:

$$\mathcal{V}(\zeta) = \sum_{j=0}^{\mathbb{M}} \mathfrak{A}_j \mathcal{G}^j(\zeta) + \sum_{j=1}^{\mathbb{M}} \mathfrak{B}_j \mathcal{G}^{-j}(\zeta), \tag{2.4}$$

here the parameters $\mathfrak{A}_j$ and $\mathfrak{B}_j$ $(j = 1, 2, ..., \mathbb{M})$ stand for constants in the solution equation that will be computed. This provides the necessary condition that neither $\mathfrak{A}_{\mathbb{M}}$ nor $\mathfrak{B}_{\mathbb{M}}$ can be zero at the same time.
Step (III): In order to assess the positive integer $\mathbb{M}$, the balancing principle (BP) is employed to Eq. (2.3). And the function $\mathcal{G}(\zeta)$ also satisfies the following constrain:

$$(\mathcal{G}'(\zeta))^2 = \left(\frac{d\mathcal{G}}{d\zeta}\right)^2 = \tau_0 + \tau_1 \mathcal{G}(\zeta) + \tau_2 \mathcal{G}^2(\zeta) + \tau_3 \mathcal{G}^3(\zeta) + \tau_4 \mathcal{G}^4(\zeta), \tag{2.5}$$

while τ_l $(0 \le l \le 4)$ represent constant values that shall assist in identifying potential solution scenarios.
By selecting different certain values of $\tau_0, \tau_1, \tau_2, \tau_3$ and τ_4, Eq. (2.5) may have the following general solutions:
Result 1: When $\tau_0 = \tau_1 = \tau_3 = 0$,

$$\mathcal{G}(\zeta) = \sqrt{-\frac{\tau_2}{\tau_4}}\,\mathrm{sech}\left[\zeta\sqrt{\tau_2}\right], \qquad \tau_2 > 0,\ \tau_4 < 0,$$

$$\mathcal{G}(\zeta) = \sqrt{-\frac{\tau_2}{\tau_4}}\,\sec\left[\zeta\sqrt{-\tau_2}\right], \qquad \tau_2 < 0,\ \tau_4 > 0.$$

Result 2: When $\tau_1 = \tau_3 = 0$,

$$\mathcal{G}(\zeta) = \sqrt{-\frac{\aleph^2\tau_2}{(2\aleph^2-1)\,\tau_4}}\,\mathrm{cn}\left[\zeta\sqrt{\frac{\tau_2}{2\aleph^2-1}}\right], \tau_2 > 0,\ \tau_4 < 0,\ \tau_0 = \frac{\aleph^2\left(1-\aleph^2\right)\tau_2^2}{4\left(2\aleph^2-1\right)^2\tau_4},$$

$$\mathcal{G}(\zeta) = \sqrt{-\frac{\aleph^2}{(2-\aleph^2)\,\tau_4}}\,\mathrm{dn}\left[\zeta\sqrt{\frac{\tau_2}{2-\aleph^2}}\right], \tau_2 > 0,\ \tau_4 < 0,\ \tau_0 = \frac{\left(1-\aleph^2\right)\tau_2^2}{\left(2-\aleph^2\right)^2\tau_4},$$

$$\mathcal{G}(\zeta) = \sqrt{-\frac{\aleph^2\tau_2}{(\aleph^2+1)\,\tau_4}}\,\mathrm{sn}\left[\zeta\sqrt{\frac{-\tau_2}{\aleph^2+1}}\right], \quad \tau_2 < 0,\ \tau_4 > 0,\ \tau_0 = \frac{\aleph^2\tau_2^2}{\left(\aleph^2+1\right)^2\tau_4}.$$

$$\mathcal{G}(\zeta) = \epsilon\sqrt{-\frac{\tau_2}{2\tau_4}}\tanh\left(\sqrt{-\frac{\tau_2}{2}}\,\zeta\right), \qquad \tau_2 < 0, \tau_4 > 0, \tau_0 = \frac{\tau_2^2}{4\tau_4},$$

$$\mathcal{G}(\zeta) = \epsilon\sqrt{\frac{\tau_2}{2\tau_4}}\tan\left(\sqrt{\frac{\tau_2}{2}}\,\zeta\right), \qquad \tau_2 > 0, \tau_4 > 0, \tau_0 = \frac{\tau_2^2}{4\tau_4},$$

where $\aleph$ is the modulus of the JEFs, $0 \le \aleph \le 1$ and $\epsilon = \pm 1$.

Result 3: When $\tau_0 = \tau_1 = \tau_4 = 0$,

$$\mathcal{G}(\zeta) = -\frac{\tau_2}{\tau_3}\sec h^2\left(\frac{\sqrt{\tau_2}}{2}\,\zeta\right), \qquad \tau_2 > 0,$$

$$\mathcal{G}(\zeta) = -\frac{\tau_2}{\tau_3}\sec^2\left(\frac{\sqrt{-\tau_2}}{2}\,\zeta\right), \qquad \tau_2 < 0.$$

Result 4: When $\tau_3 = \tau_4 = 0$,

$$\mathcal{G}(\zeta) = -\frac{\tau_1}{2\tau_2} + \exp\left(\epsilon\sqrt{\tau_2}\,\zeta\right), \qquad \tau_2 > 0, \tau_0 = \frac{\tau_1^2}{4\tau_2},$$

$$\mathcal{G}(\zeta) = -\frac{\tau_1}{2\tau_2} + \frac{\epsilon\tau_1}{2\tau_2}\sin\left(\sqrt{-\tau_2}\,\zeta\right), \qquad \tau_0 = 0, \tau_2 < 0,$$

$$\mathcal{G}(\zeta) = -\frac{\tau_1}{2\tau_2} + \frac{\epsilon\tau_1}{2\tau_2}\sinh\left(2\sqrt{\tau_2}\,\zeta\right), \qquad \tau_0 = 0, \tau_2 > 0,$$

$$\mathcal{G}(\zeta) = \epsilon\sqrt{-\frac{\tau_0}{\tau_2}}\sin\left(\sqrt{-\tau_2}\,\zeta\right), \qquad \tau_1 = 0, \tau_0 > 0, \tau_2 < 0,$$

$$\mathcal{G}(\zeta) = \epsilon\sqrt{\frac{\tau_0}{\tau_2}}\sinh\left(\sqrt{\tau_2}\,\zeta\right), \qquad \tau_1 = 0, \tau_0 > 0, \tau_2 > 0.$$

Result 5: When $\tau_0 = \tau_1 = 0,\ \tau_4 > 0,$

$$\mathcal{G}(\zeta) = -\frac{\tau_2 \sec^2\left(\frac{\sqrt{-\tau_2}}{2}\,\zeta\right)}{2\varepsilon\sqrt{-\tau_2\tau_4}\tan\left(\frac{\sqrt{-\tau_2}}{2}\,\zeta\right) + \tau_3}, \qquad \tau_2 < 0,$$

$$\mathcal{G}(\zeta) = \frac{\tau_2 \sec h^2\left(\frac{\sqrt{\tau_2}}{2}\,\zeta\right)}{2\varepsilon\sqrt{\tau_2\tau_4}\tanh\left(\frac{\sqrt{\tau_2}}{2}\,\zeta\right) - \tau_3}, \qquad \tau_2 > 0, \tau_3 \neq 2\varepsilon\sqrt{\tau_2\tau_4},$$

$$\mathcal{G}(\zeta) = \frac{1}{2}\varepsilon\sqrt{\frac{\tau_2}{\tau_4}}\left(1 + \tanh\left(\frac{\sqrt{\tau_2}}{2}\,\zeta\right)\right), \qquad \tau_2 > 0, \tau_3 = 2\varepsilon\sqrt{\tau_2\tau_4}.$$

Step (IV): Rendering Eq. (2.3) with the solution that seems to be provided in Eqs. (2.4) and (2.5) will generate a polynomial in $\mathcal{G}(\zeta)$. Mathematical software like Wolfram Mathematica or Maple programs may be utilized to solve an algebraic system of non-linear equations that arises when the coefficients of $\mathcal{G}^k(\zeta)$, $(k = 0, \pm1, \pm2, ...)$, are set equal to zero. For the traveling wave in Eq. (2.1), there are thus several exact solutions that we can obtain.

The following table represents a comparison between the implemented methodology and the other analytical methods.

TABLE 1. Comparison of the IME Tanh Function method with other analytical techniques

Method	Solution Types	Symbolic Complexity	Computational Tools	Flexibility
IME Tanh method	Solitons, periodic, many other types	High	Maple, Mathematica	High
Variational Method	Approximate soliton-like	Low–Medium	Optional	Medium
Hamiltonian-based Method	Conservative wave structures	Medium	Optional	Medium
Wang's Direct Mapping Method	Exact soliton and wave solutions	Low	Optional	High
G'/G Expansion Method	Soliton, exponential, rational	Medium	Maple, Mathematica	Medium
Sine-Cosine Method	Periodic, solitary	Low–Medium	Optional	Medium
Tanh-Coth Method	Solitary wave, shock	Medium	Maple, Mathematica	Medium

3. Stochastic soliton solutions retrieval

In this part, the IME tanh function algorithm is utilized to create all possible solutions for Eq. (1.1). To achieve this, we utilize the transformation shown below:

$$\psi(x, y, t) = \mathcal{H}(\zeta)e^{i\left(-\ell x + ky + \omega t + \varrho W(t) - \varrho^2 t\right)}, \qquad \zeta = x + y - \vartheta t, \tag{3.1}$$

where $\mathcal{H}(\zeta)$ denotes the amplitude part of the solution and ℓ, k, ω, ϑ are certain constant parameters. When (3.1) is substituted into Eq. (1.1) and the real and imaginary parts could be separated, respectively, to yield

$$(\eta_1 + \eta_2 + \eta_3)\,\mathcal{H}'' - \left(\eta_2 k^2 - \eta_3 k\ell + \omega + \eta_1\ell^2 - \varrho^2\right)\mathcal{H} - \eta_4\mathcal{H}^3 = 0, \tag{3.2}$$

$$\left(-2\eta_2 k+\eta_3(\ell-k)+2\eta_1\ell+\vartheta\right)\mathcal{H}'=0. \tag{3.3}$$

After vanishing the coefficient of $\mathcal{H}'$ in Eq. (3.3), one can obtain the soliton velocity as:

$$\vartheta=-\left(-2\eta_2 k+\eta_3(\ell-k)+2\eta_1\ell\right). \tag{3.4}$$

Therefore, using the BP described in section 2 between $\mathcal{H}''$ and $\mathcal{H}^3$, we may establish the exact solution form for Eq. (3.2), as follows:

$$\mathcal{H}(\zeta)=\mathfrak{A}_0+\mathfrak{A}_1\mathcal{G}(\zeta)+\frac{\mathfrak{B}_1}{\mathcal{G}(\zeta)}. \tag{3.5}$$

If the solution form in Eq. (3.5) is replaced with the limitation in Eq. (2.5), then there exists a polynomial in $\mathcal{G}(\zeta)$ resulting from the substitution in Eq. (3.2). When all terms with the same powers are added together and eventually equal to zero, an algebraic system of nonlinear equations is produced, which will be

$$\begin{aligned}
0&=-\eta_2 k^2\mathfrak{A}_0+\eta_3 k\ell\mathfrak{A}_0-\eta_1\ell^2\mathfrak{A}_0+\frac{1}{2}\eta_1\tau_1\mathfrak{A}_1+\frac{1}{2}\eta_2\tau_1\mathfrak{A}_1+\frac{1}{2}\eta_3\tau_1\mathfrak{A}_1-\eta_4\mathfrak{A}_0^3-\omega\mathfrak{A}_0-6\eta_4\mathfrak{A}_1\mathfrak{A}_0\mathfrak{B}_1\\
&\quad+\mathfrak{A}_0\varrho^2+\frac{1}{2}\eta_1\tau_3\mathfrak{B}_1+\frac{1}{2}\eta_2\tau_3\mathfrak{B}_1+\frac{1}{2}\eta_3\tau_3\mathfrak{B}_1,\\
0&=2\eta_1\tau_0\mathfrak{B}_1+2\eta_2\tau_0\mathfrak{B}_1+2\eta_3\tau_0\mathfrak{B}_1-\eta_4\mathfrak{B}_1^3,\\
0&=-3\eta_4\mathfrak{A}_0\mathfrak{B}_1^2+\frac{3}{2}\eta_1\tau_1\mathfrak{B}_1+\frac{3}{2}\eta_2\tau_1\mathfrak{B}_1+\frac{3}{2}\eta_3\tau_1\mathfrak{B}_1,\\
0&=-\eta_2 k^2\mathfrak{B}_1+\eta_3 k\ell\mathfrak{B}_1-\eta_1\ell^2\mathfrak{B}_1-3\eta_4\mathfrak{A}_1\mathfrak{B}_1^2-3\eta_4\mathfrak{A}_0^2\mathfrak{B}_1+\eta_1\tau_2\mathfrak{B}_1+\eta_2\tau_2\mathfrak{B}_1+\eta_3\tau_2\mathfrak{B}_1-\omega\mathfrak{B}_1+\mathfrak{B}_1\varrho^2,\\
0&=-\eta_2 k^2\mathfrak{A}_1+\eta_3 k\ell\mathfrak{A}_1-\eta_1\ell^2\mathfrak{A}_1+\eta_1\tau_2\mathfrak{A}_1+\eta_2\tau_2\mathfrak{A}_1+\eta_3\tau_2\mathfrak{A}_1-3\eta_4\mathfrak{A}_0^2\mathfrak{A}_1-\omega\mathfrak{A}_1-3\eta_4\mathfrak{A}_1^2\mathfrak{B}_1+\mathfrak{A}_1\varrho^2,\\
0&=\frac{3}{2}\eta_1\tau_3\mathfrak{A}_1+\frac{3}{2}\eta_2\tau_3\mathfrak{A}_1+\frac{3}{2}\eta_3\tau_3\mathfrak{A}_1-3\eta_4\mathfrak{A}_0\mathfrak{A}_1^2,\\
0&=2\eta_1\tau_4\mathfrak{A}_1+2\eta_2\tau_4\mathfrak{A}_1+2\eta_3\tau_4\mathfrak{A}_1-\eta_4\mathfrak{A}_1^3.
\end{aligned} \tag{3.6}$$

Solving these equations in (3.6) with the Wolfram Mathematica program allows us to get the following results, but satisfying the condition that $\mathfrak{A}_1$ and $\mathfrak{B}_1$ cannot both be zero simultaneously.

Result (1) : If $\tau_0=\tau_1=\tau_3=0$, then we got

$$\mathfrak{A}_0=\mathfrak{B}_1=0,\ \mathfrak{A}_1=\pm\sqrt{\frac{2\left(\eta_1+\eta_2+\eta_3\right)\tau_4}{\eta_4}},\ \tau_2=\frac{\eta_2 k^2-\eta_3 k\ell+\omega+\eta_1\ell^2-\varrho^2}{\eta_1+\eta_2+\eta_3}.$$

By considering the raised set, Eq. (1.1) has the following solutions:

(1.1): If $\tau_2>0,\ \tau_4<0$, so:

$$\psi_{1.1}(x,y,t)=\pm\sqrt{-\frac{2\left(\eta_1+\eta_2+\eta_3\right)\tau_2}{\eta_4}}\operatorname{sech}\left[(x+y-\vartheta t)\sqrt{\tau_2}\right]e^{i\left(-\ell x+ky+\omega t+\varrho W(t)-\varrho^2 t\right)}, \tag{3.7}$$

that denotes a bright soliton solution under the condition that $\eta_4\left(\eta_1+\eta_2+\eta_3\right)<0$.

(1.2): If $\tau_2<0,\ \tau_4>0$, so:

$$\psi_{1.2}(x,y,t)=\pm\sqrt{-\frac{2\left(\eta_1+\eta_2+\eta_3\right)\tau_2}{\eta_4}}\sec\left[(x+y-\vartheta t)\sqrt{-\tau_2}\right]e^{i\left(-\ell x+ky+\omega t+\varrho W(t)-\varrho^2 t\right)}, \tag{3.8}$$

that describes a singular periodic solution when satisfying the constraint $\eta_4\left(\eta_1+\eta_2+\eta_3\right)>0$.

(1.3): If $\tau_2=0,\ \tau_4>0$, so:

$$\psi_{1.3}(x,y,t)=-\frac{\sqrt{\frac{2\left(\eta_1+\eta_2+\eta_3\right)}{\eta_4}}}{x+y-\vartheta t}e^{i\left(-\ell x+ky+\omega t+\varrho W(t)-\varrho^2 t\right)}, \tag{3.9}$$

which denotes a rational solution when satisfying the constraint $\eta_4\left(\eta_1+\eta_2+\eta_3\right)>0$.

Result (2) : If $\tau_1=\tau_3=0$, then

(2.1): $\mathfrak{A}_0=\mathfrak{B}_1=0,\ \mathfrak{A}_1=\pm\sqrt{\dfrac{2\left(\eta_1+\eta_2+\eta_3\right)\tau_4}{\eta_4}},\ \tau_2=\dfrac{\eta_2k^2-\eta_3k\ell+\omega+\eta_1\ell^2-\varrho^2}{\eta_1+\eta_2+\eta_3}.$

(2.2): $\mathfrak{A}_0=\mathfrak{A}_1=0,\ \mathfrak{B}_1=\pm\sqrt{\dfrac{2\left(\eta_1+\eta_2+\eta_3\right)\tau_0}{\eta_4}},\ \tau_2=\dfrac{\eta_2k^2-\eta_3k\ell+\omega+\eta_1\ell^2-\varrho^2}{\eta_1+\eta_2+\eta_3}.$

Considering set (2.1), Eq. (1.1) has the following solutions:

(2.1,1): If $\tau_2<0,\ \tau_4>0$, and $\tau_0=\frac{\tau_2^2}{4\tau_4}$, then:

$$\psi_{2.1,1}(x,y,t)=\sqrt{-\frac{\left(\eta_1+\eta_2+\eta_3\right)\tau_2}{\eta_4}}\tanh\left[(x+y-\vartheta t)\sqrt{-\frac{\tau_2}{2}}\right]e^{i\left(-\ell x+ky+\omega t+\varrho W(t)-\varrho^2t\right)},\tag{3.10}$$

and it is considered as a dark soliton solution such that $\eta_4\left(\eta_1+\eta_2+\eta_3\right)>0$.

(2.1,2): If $\tau_2>0,\ \tau_4>0$, and $\tau_0=\frac{\tau_2^2}{4\tau_4}$, then:

$$\psi_{2.1,2}(x,y,t)=\sqrt{\frac{\left(\eta_1+\eta_2+\eta_3\right)\tau_2}{\eta_4}}\tan\left[(x+y-\vartheta t)\sqrt{\frac{\tau_2}{2}}\right]e^{i\left(-\ell x+ky+\omega t+\varrho W(t)-\varrho^2t\right)},\tag{3.11}$$

that is a singular periodic solution such that $\eta_4\left(\eta_1+\eta_2+\eta_3\right)>0$.

(2.1,3): If $\tau_2>0,\ \tau_4<0,\ \tau_0=\frac{\aleph^2\left(1-\aleph^2\right)\tau_2^2}{\left(2\aleph^2-1\right)^2\tau_4}$, and $0<\aleph\leq1$, a JEF solution is raised provided that $\aleph\neq\dfrac{1}{\sqrt{2}}$ and $\eta_4\left(\eta_1+\eta_2+\eta_3\right)<0$:

$$\psi_{2.1,3}(x,y,t)=\pm\aleph\sqrt{\frac{2\left(\eta_1+\eta_2+\eta_3\right)\tau_2}{\eta_4\left(1-2\aleph^2\right)}}\mathrm{cn}(x+y-\vartheta t)e^{i\left(-\ell x+ky+\omega t+\varrho W(t)-\varrho^2t\right)},\tag{3.12}$$

when setting $\aleph=1$, a bright soliton solution can be raised as:

$$\psi_{2.1,4}(x,y,t)=\pm\sqrt{-\frac{2\left(\eta_1+\eta_2+\eta_3\right)\tau_2}{\eta_4}}\mathrm{sech}[x+y-\vartheta t]e^{i\left(-\ell x+ky+\omega t+\varrho W(t)-\varrho^2t\right)}.\tag{3.13}$$

(2.1,4): If $\tau_2>0,\ \tau_4<0,\ \tau_0=\frac{\left(1-\aleph^2\right)\tau_2^2}{\left(2-\aleph^2\right)^2\tau_4},\ \eta_4\left(\eta_1+\eta_2+\eta_3\right)<0$, and $0<\aleph\leq1$, a JEF solution is constructed as:

$$\psi_{2.1,5}(x,y,t)=\pm\aleph\sqrt{-\frac{2\left(\eta_1+\eta_2+\eta_3\right)}{\eta_4\left(2-\aleph^2\right)}}\mathrm{dn}(x+y-\vartheta t)e^{i\left(-\ell x+ky+\omega t+\varrho W(t)-\varrho^2t\right)},\tag{3.14}$$

when setting $\aleph=1$, a bright soliton solution can be raised as:

$$\psi_{2.1,6}(x,y,t)=\pm\sqrt{-\frac{2\left(\eta_1+\eta_2+\eta_3\right)}{\eta_4}}\mathrm{sech}[x+y-\vartheta t]e^{i\left(-\ell x+ky+\omega t+\varrho W(t)-\varrho^2t\right)}.\tag{3.15}$$

(2.1,5): If $\tau_2<0,\ \tau_4>0,\ \tau_0=\frac{\aleph^2\tau_2^2}{\left(1+\aleph^2\right)^2\tau_4},\ \eta_4\left(\eta_1+\eta_2+\eta_3\right)>0$, and $0<\aleph\leq1$, a JEF solution is raised as:

$$\psi_{2.1,7}(x,y,t)=\aleph\sqrt{-\frac{2\left(\eta_1+\eta_2+\eta_3\right)\tau_2}{\eta_4\left(\aleph^2+1\right)}}\mathrm{sn}(x+y-\vartheta t)e^{i\left(-\ell x+ky+\omega t+\varrho W(t)-\varrho^2t\right)},\tag{3.16}$$

when setting $\aleph=1$, we find a dark soliton solution:

$$\psi_{2.1,8}(x,y,t)=\sqrt{-\frac{\left(\eta_1+\eta_2+\eta_3\right)\tau_2}{\eta_4}}\tanh[x+y-\vartheta t]e^{i\left(-\ell x+ky+\omega t+\varrho W(t)-\varrho^2t\right)}.\tag{3.17}$$

Considering the set (2.2), the solutions of Eq. (1.1) will be:

(2.2,1): If $\tau_2 < 0,\ \tau_4 > 0$, and $\tau_0 = \frac{\tau_2^2}{4\tau_4}$, then:

$$\psi_{2.2,1}(x,y,t) = \sqrt{-\frac{(\eta_1+\eta_2+\eta_3)\,\tau_2}{\eta_4}}\coth\left[(x+y-\vartheta t)\sqrt{-\frac{\tau_2}{2}}\right]e^{i\left(-\ell x+ky+\omega t+\varrho W(t)-\varrho^2 t\right)}, \tag{3.18}$$

which is a singular soliton solution provided that $\eta_4\,(\eta_1+\eta_2+\eta_3) > 0$.

(2.2,2): If $\tau_2 > 0,\ \tau_4 > 0$, and $\tau_0 = \frac{\tau_2^2}{4\tau_4}$, then:

$$\psi_{2.2,2}(x,y,t) = \sqrt{\frac{(\eta_1+\eta_2+\eta_3)\,\tau_2}{\eta_4}}\cot\left[(x+y-\vartheta t)\sqrt{\frac{\tau_2}{2}}\right]e^{i\left(-\ell x+ky+\omega t+\varrho W(t)-\varrho^2 t\right)}, \tag{3.19}$$

that is a singular periodic solution such that $\eta_4\,(\eta_1+\eta_2+\eta_3) > 0$.

(2.2,3): If $\tau_2 > 0,\ \tau_4 < 0,\ \tau_0 = \frac{\aleph^2(1-\aleph^2)\tau_2^2}{(2\aleph^2-1)^2\tau_4}$, and $0 \le \aleph < 1$, a JEF solution is raised provided that $\aleph \neq \frac{1}{\sqrt{2}}$ and $\eta_4\,(\eta_1+\eta_2+\eta_3) > 0$:

$$\psi_{2.2,3}(x,y,t) = \pm\sqrt{-\frac{2\,(\eta_1+\eta_2+\eta_3)\,(1-\aleph^2)\,\tau_2}{\eta_4\,(2\aleph^2-1)}}\,\mathrm{nc}(x+y-\vartheta t)e^{i\left(-\ell x+ky+\omega t+\varrho W(t)-\varrho^2 t\right)}, \tag{3.20}$$

when setting $\aleph = 0$, we find a singular periodic solution:

$$\psi_{2.2,4}(x,y,t) = \pm\sqrt{\frac{2\,(\eta_1+\eta_2+\eta_3)\,\tau_2}{\eta_4}}\,\sec[x+y-\vartheta t]e^{i\left(-\ell x+ky+\omega t+\varrho W(t)-\varrho^2 t\right)}. \tag{3.21}$$

(2.2,4): If $\tau_2 > 0,\ \tau_4 < 0,\ \tau_0 = \frac{(1-\aleph^2)\tau_2^2}{(2-\aleph^2)^2\tau_4},\ \eta_4\,(\eta_1+\eta_2+\eta_3) > 0$, and $0 < \aleph < 1$, a JEF solution is constructed as:

$$\psi_{2.2,5}(x,y,t) = \pm\aleph\,\tau_2\sqrt{-\frac{2\,(\eta_1+\eta_2+\eta_3)\,(1-\aleph^2)}{\eta_4\,(2-\aleph^2)}}\,\mathrm{nd}(x+y-\vartheta t)e^{i\left(-\ell x+ky+\omega t+\varrho W(t)-\varrho^2 t\right)}. \tag{3.22}$$

(2.2,5): If $\tau_2 < 0,\ \tau_4 > 0,\ \tau_0 = \frac{\aleph^2\tau_2^2}{(1+\aleph^2)^2\tau_4},\ \eta_4\,(\eta_1+\eta_2+\eta_3) > 0$, and $0 \le \aleph \le 1$, a JEF solution is raised as:

$$\psi_{2.2,6}(x,y,t) = \sqrt{-\frac{2\,(\eta_1+\eta_2+\eta_3)\,\tau_2}{\eta_4\,(\aleph^2+1)}}\,\mathrm{ns}(x+y-\vartheta t)e^{i\left(-\ell x+ky+\omega t+\varrho W(t)-\varrho^2 t\right)}, \tag{3.23}$$

when setting either $\aleph = 0$ or $\aleph = 1$, we find either a singular periodic solution or a singular soliton solution, respectively, as:

$$\psi_{2.2,7}(x,y,t) = \sqrt{-\frac{2\,(\eta_1+\eta_2+\eta_3)\,\tau_2}{\eta_4}}\,\csc[x+y-\vartheta t]e^{i\left(-\ell x+ky+\omega t+\varrho W(t)-\varrho^2 t\right)}, \tag{3.24}$$

$$\psi_{2.2,8}(x,y,t) = \sqrt{-\frac{(\eta_1+\eta_2+\eta_3)\,\tau_2}{\eta_4}}\,\coth[x+y-\vartheta t]e^{i\left(-\ell x+ky+\omega t+\varrho W(t)-\varrho^2 t\right)}, \tag{3.25}$$

Result (3) : If $\tau_2 = \tau_4 = 0,\ \tau_0 \neq 0,\ \tau_1 \neq 0$ and $\tau_3 > 0$, then

$$\mathfrak{A}_0 = \pm\frac{\tau_1\sqrt{\varrho^2-\omega}}{\sqrt{\eta_4\,(3\tau_1^2+8\tau_0\ell^2)}},\ \mathfrak{A}_1 = 0,\ \mathfrak{B}_1 = \pm\frac{4\tau_0\sqrt{\varrho^2-\omega}}{\sqrt{\eta_4\,(3\tau_1^2+8\tau_0\ell^2)}},\ \tau_3 = -\frac{\tau_1^3}{8\tau_0^2},\ k = -\ell,\ \eta_1 = -\eta_2-\eta_3+\frac{8\tau_0\,(\varrho^2-\omega)}{3\tau_1^2+8\tau_0\ell^2}.$$

Using the obtained set, one shall obtain Weierstrass elliptic doubly periodic type solutions as:

$$\psi_3(x,y,t) = \sqrt{\frac{\varrho^2-\omega}{\eta_4\,(3\tau_1^2+8\tau_0\ell^2)}}\left(\frac{4\tau_0}{\wp\left(\frac{1}{2}(x+y-\vartheta t)\sqrt{\tau_3};-\frac{4\tau_1}{\tau_3},-\frac{4\tau_0}{\tau_3}\right)}+\tau_1\right)e^{i\left(-\ell x+ky+\omega t+\varrho W(t)-\varrho^2 t\right)}, \tag{3.26}$$

provided that $\left(\varrho^2-\omega\right)\left(\eta_4\left(3\tau_1^2+8\tau_0\ell^2\right)\right)>0$.

Result (4) : If $\tau_3=\tau_4=0$, then, in this case, we find:

(4.1): $\mathfrak{A}_0=0,\ \mathfrak{A}_1=\tau_1=0,\ \mathfrak{B}_1=\pm\sqrt{\dfrac{2\left(\eta_1+\eta_2+\eta_3\right)\tau_0}{\eta_4}},\ \omega=\left(\eta_1+\eta_2+\eta_3\right)\tau_2-\eta_2k^2+\eta_3k\ell-\eta_1\ell^2+\varrho^2.$

(4.2): $\mathfrak{A}_1=0,\ \mathfrak{B}_1=\pm2\mathfrak{A}_0\sqrt{\dfrac{\tau_0}{\tau_2}},\ \tau_1=\pm2\sqrt{\tau_0\tau_2},\ \eta_4=\dfrac{\left(\eta_1+\eta_2+\eta_3\right)\tau_2}{2\mathfrak{A}_0^2},\ \omega=-\dfrac{1}{2}\left(\eta_1+\eta_2+\eta_3\right)\tau_2-\eta_2k^2+\eta_3k\ell-\eta_1\ell^2+\varrho^2.$

From the set (4.1), we can construct the upcoming solutions such that $\eta_4\left(\eta_1+\eta_2+\eta_3\right)>0$:

(4.1,1): If $\tau_0>0$ and $\tau_2<0$, the following singular periodic solution shall be retrieved:

$$\psi_{4.1,1}(x,y,t)=\sqrt{-\frac{2\left(\eta_1+\eta_2+\eta_3\right)\tau_2}{\eta_4}}\csc\left[(x+y-\vartheta t)\sqrt{-\tau_2}\right]e^{i\left(-\ell x+ky+\omega t+\varrho W(t)-\varrho^2t\right)}. \tag{3.27}$$

(4.1,2): If $\tau_0>0$ and $\tau_2>0$, the following singular soliton solution will be found:

$$\psi_{4.1,2}(x,y,t)=\sqrt{\frac{2\left(\eta_1+\eta_2+\eta_3\right)\tau_2}{\eta_4}}\operatorname{csch}\left[(x+y-\vartheta t)\sqrt{\tau_2}\right]e^{i\left(-\ell x+ky+\omega t+\varrho W(t)-\varrho^2t\right)}. \tag{3.28}$$

From the set (4.2), we may build the next exponential solution as follows:

$$\psi_{4.2}(x,y,t)=\mathfrak{A}_0\left(1-\frac{\tau_1\pm2}{\tau_1-2\tau_2e^{\sqrt{\tau_2}(x+y-\vartheta t)}}\right)e^{i\left(-\ell x+ky+\omega t+\varrho W(t)-\varrho^2t\right)}, \tag{3.29}$$

provided that $\tau_2>0$ and $\tau_1-2\tau_2e^{\sqrt{\tau_2}(x+y-\vartheta t)}\neq0$.

Result (5) : If $\tau_0=\tau_1=0$ and $\tau_4>0$, then we obtain:

$$\mathfrak{A}_0=\mathfrak{B}_1=\tau_3=0,\ \mathfrak{A}_1=\pm\sqrt{-\frac{2\tau_4\left((k+\ell)\left(\eta_2(\ell-k)+\eta_3\ell\right)-\omega+\varrho^2\right)}{\eta_4\left(\tau_2-\ell^2\right)}},\ \eta_1=\frac{\eta_2\left(\tau_2-k^2\right)+\eta_3\left(k\ell+\tau_2\right)-\omega+\varrho^2}{\ell^2-\tau_2}.$$

which gives either a singular periodic solution or a singular soliton solution by providing that $\eta_4\left(\ell^2-\tau_2\right)\left((k+\ell)\left(\eta_2(\ell-k)+\eta_3\ell\right)-\right.$ $\left.0\right.$:

$$\psi_{5.1}(x,y,t)=-\sqrt{-\frac{2\tau_2\left((k+\ell)\left(\eta_2(\ell-k)+\eta_3\ell\right)-\omega+\varrho^2\right)}{\eta_4\left(\ell^2-\tau_2\right)}}\csc\left[(x+y-\vartheta t)\sqrt{-\tau_2}\right]$$
$$\times e^{i\left(-\ell x+ky+\omega t+\varrho W(t)-\varrho^2t\right)},\qquad \tau_2<0, \tag{3.30}$$

$$\psi_{5.2}(x,y,t)=\sqrt{\frac{2\tau_2\left((k+\ell)\left(\eta_2(\ell-k)+\eta_3\ell\right)-\omega+\varrho^2\right)}{\eta_4\left(\ell^2-\tau_2\right)}}\operatorname{csch}\left[(x+y-\vartheta t)\sqrt{\tau_2}\right]$$
$$\times e^{i\left(-\ell x+ky+\omega t+\varrho W(t)-\varrho^2t\right)},\qquad \tau_2>0. \tag{3.31}$$

4. White noise influence on the extracted solutions

Changing the parameter values in the model under study allowed for the extraction of many categories of solutions for Eq. (1.1). This technique has therefore been used to produce some incredible outcomes that have never been documented or attained. Sketches of several particular solutions that the two- and three-dimensional simulation produced highlight the physical properties of the recovered solutions. These graphical simulations will show how robust the higher solutions are against perturbations, and they are made using MATLAB software. In Figure 1, we showed the real part of Eq. (3.7) along the $x-$direction in a three-dimensional plot by using different noise strengths when the parameters are $\eta_1=0.5,\ \eta_2=0.6,\ \eta_3=0.7,\ \eta_4=-0.8,\ \omega=0.7,\ k=0.8,\ \ell=1,$ while $-10\leq x\leq10$. In addition, fig. 2 displays a collective two-dimensional plot that represents all sketched plots with different noise intensities for Eq. (3.7). It demonstrates how increasing the noise intensity ϱ leads to significant distortion and broadening of the

solution profile, indicating a strong sensitivity of the system to stochastic perturbations. As ϱ increases, the real part of the wavefunction deviates from its original solitonic shape, exhibiting irregular fluctuations and reduced coherence in the spatial domain. In Figure 3, we displayed the real part of Eq. (3.7) along the $y-$direction in a three-dimensional plot by using different noise strengths when the parameters take the same values from fig. 1 but $-10 \leq y \leq 10$. Figure 4 displays a collective two-dimensional plot that represents all sketched plots with different noise intensities for the same equation. It has been observed that the surface flattens and the level of the signal diminishes. In Figure 5, we depicted the real part of Eq. (3.10) along the $x-$direction in a three-dimensional plot by using different noise strengths when the parameters are $\eta_1 = 0.7,\ \eta_2 = -0.8,\ \eta_3 = -0.9,\ \eta_4 = -0.8,\ \omega = 0.8,\ k = 0.9,\ \ell = 0.8,$ while $-10 \leq x \leq 10$. In addition, fig. 6 displays a collective two-dimensional plot that represents all sketched plots with different noise intensities for Eq. (3.10). It is clear that, as ϱ increases, the originally smooth and periodic wave profile becomes increasingly distorted, indicating that higher noise intensities significantly disrupt the wave coherence and lead to more irregular oscillatory behavior. In Figure 7, we displayed the real part of Eq. (3.10) along the $y-$direction in a three-dimensional plot by using different noise strengths when the parameters take the same values from fig. 5 but $-10 \leq y \leq 10$. Figure 8 displays a collective two-dimensional plot that represents all sketched plots with different noise intensities for the same equation.

5. Discussion about the results

5.1. **Novelties of the study.** We effectively find accurate analytical solutions of the nonlinear (2+1)-dimensional HFSCE in this work by using the IME tanh function approach. The approach produces a wide range of novel and unreported solution configurations. We are aware of no previous presentation of these exact solutions for this problem, especially the innovative single-soliton structures. An important addition to the analytical analysis of higher-dimensional nonlinear evolution equations, the solutions' uniqueness and variety demonstrate the IME tanh approach's power.

5.2. **Physical interpretation of the obtained solutions.** In the following few lines, we provide a brief description of each solution type obtained.

- Jacobi elliptic function (JEF) solution: depicts periodic spin wave trains, in which the wave profile repeats in space or time and seamlessly transitions into soliton forms when the elliptic modulus changes.
- Bright solitons: correlate to localized spin excitations with concentrated energy, demonstrating that stable, particle-like spin-wave packets propagate in a ferromagnetic medium.
- Dark solitons: reflect localized dips in magnetization and are frequently regarded as phase-shifted disturbances buried in a continuous spin background.
- Singular solitons and rational solutions: indicate spatial blow-up behaviors or highly localized structures that may correspond to instabilities or energy concentration during noise disruption.
- Exponential solutions: illustrate decaying or amplifying spin modes, depending on the sign of the exponential factor, and can represent gain/loss effects in open magnetic systems.

6. Conclusion and future work

To produce novel kinds of soliton solutions for the suggested model in (1.1), the IME tanh function algorithm was applied for the first time with perfect results in the framework of the methods known in the literature. Exact solutions to the (2+1)-dimensional SHFSCE are demonstrated by the soliton solutions that have been attained. Studying the nonlinear spin dynamics in magnetic materials is made possible by the resultant sample of the attained solutions. The solutions obtained have a large range of physical applications in managing spin dynamics in magnetic materials and high-frequency wave transmission in quiet environments. In this work, we have effectively employed the IME tanh function algorithm to provide a wide range of exact solutions for SHFSCE under different family scenarios. These novel complex soliton solutions determined the dynamical behaviors through simulations of 2D and 3D wave profiles by selecting the optimal values for the constant parameters. The technique used yields a large number of single periodic solutions that are unique, such as JEFs, exponential, rational, singular periodic, and (bright, dark, singular) solitons. Our article has the greatest number of answers when compared with what exists in the literature.

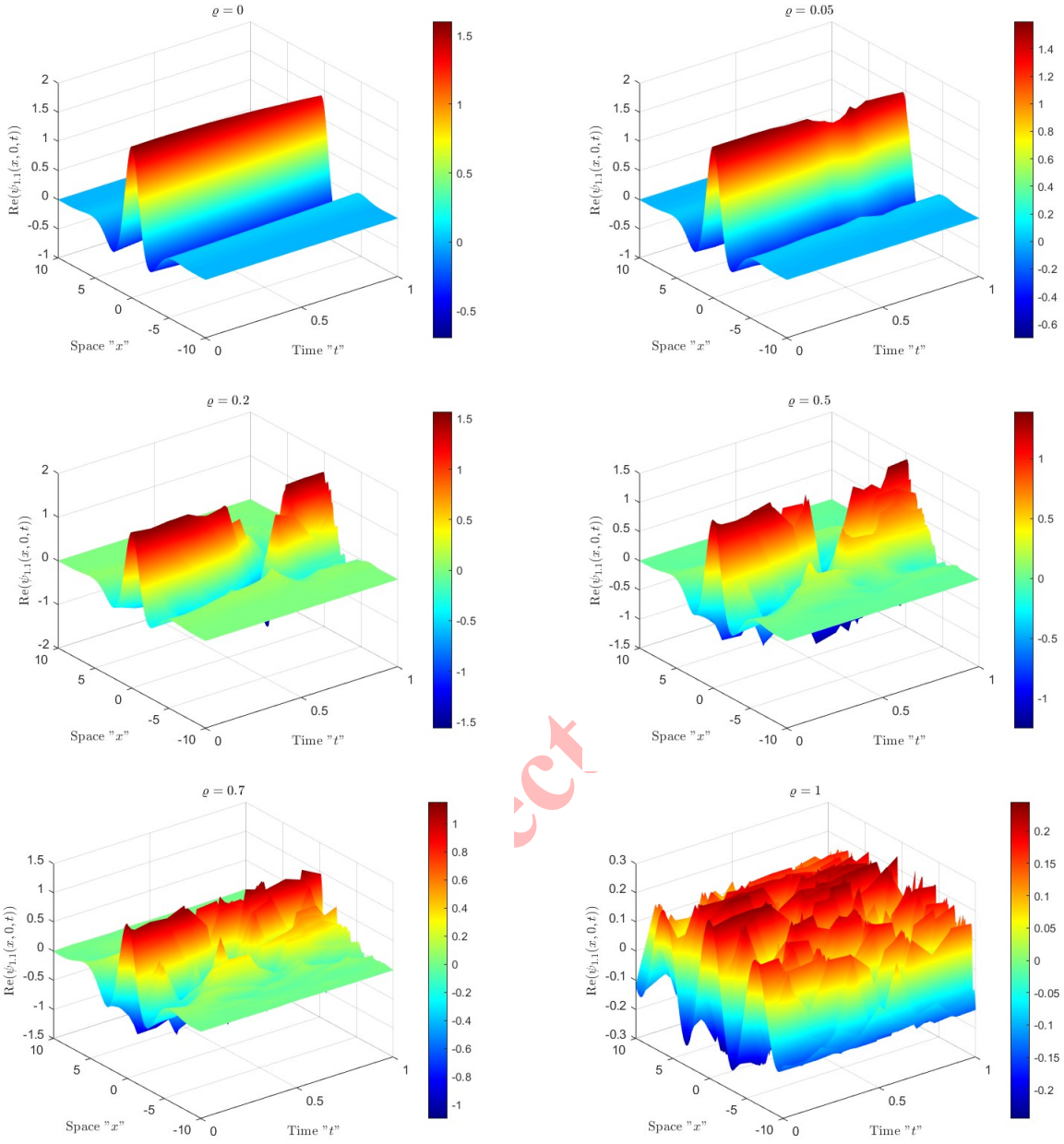

FIGURE 1. Three-dimensional plots of the real part of Eq. (3.7) along the $x-$direction with different noise intensities.

Prospectively, future studies can concentrate on investigating the stability and long-term features of the found solitary wave solutions. Investigating parametric changes and their effects on the system dynamics may reveal more intriguing events. Combining analytical and numerical approaches might lead to a deeper understanding of this complex subject. In conclusion, the whole text's results persuasively demonstrate how effective and potent the IME tanh function technique mentioned above is at precisely solving NLEEs both now and in the future.

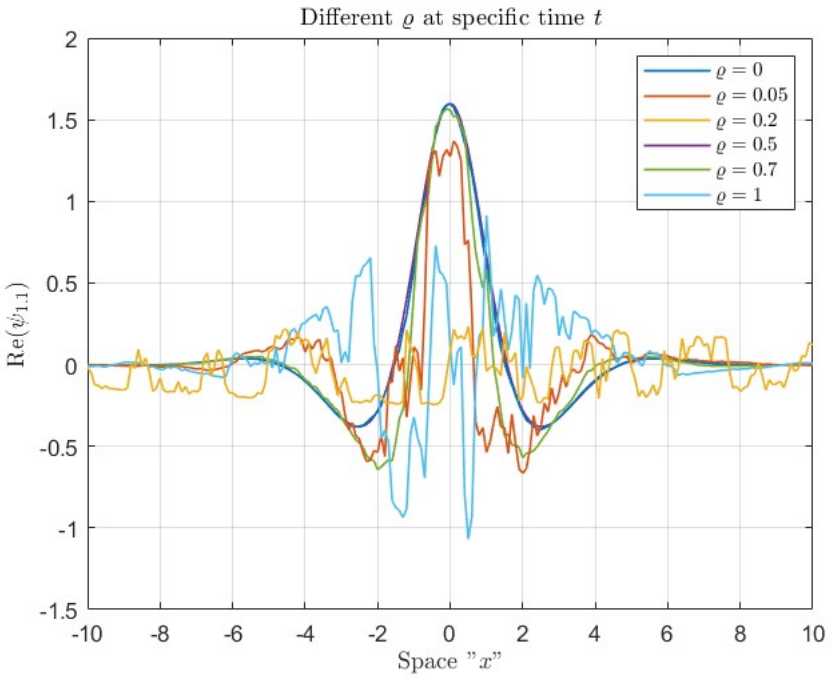

FIGURE 2. Collective two-dimensional plot the real part of Eq. (3.7) along the $x-$direction with different noise intensities.

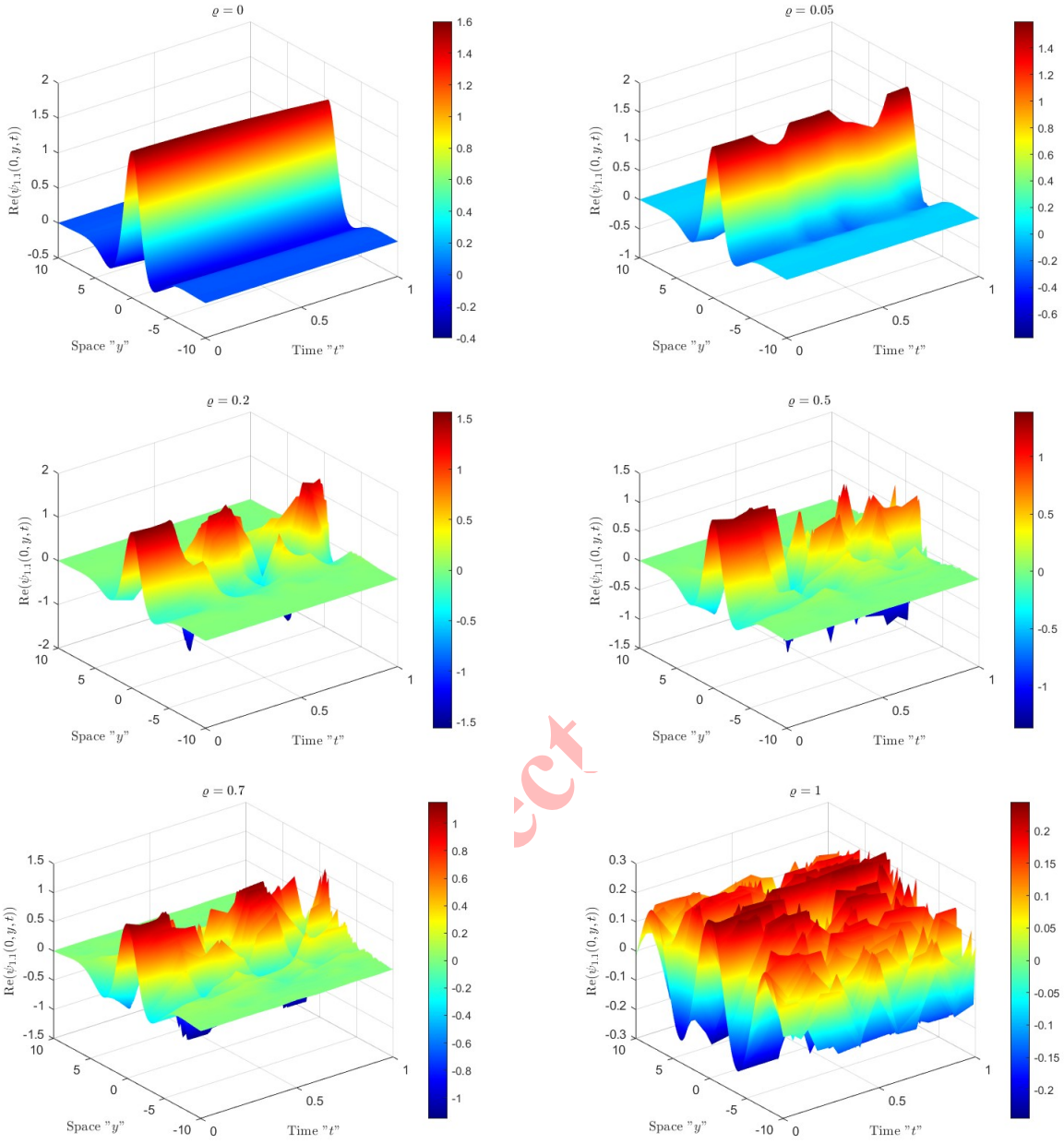

FIGURE 3. Three-dimensional plots of the real part of Eq. (3.7) along the $y-$direction with different noise intensities.

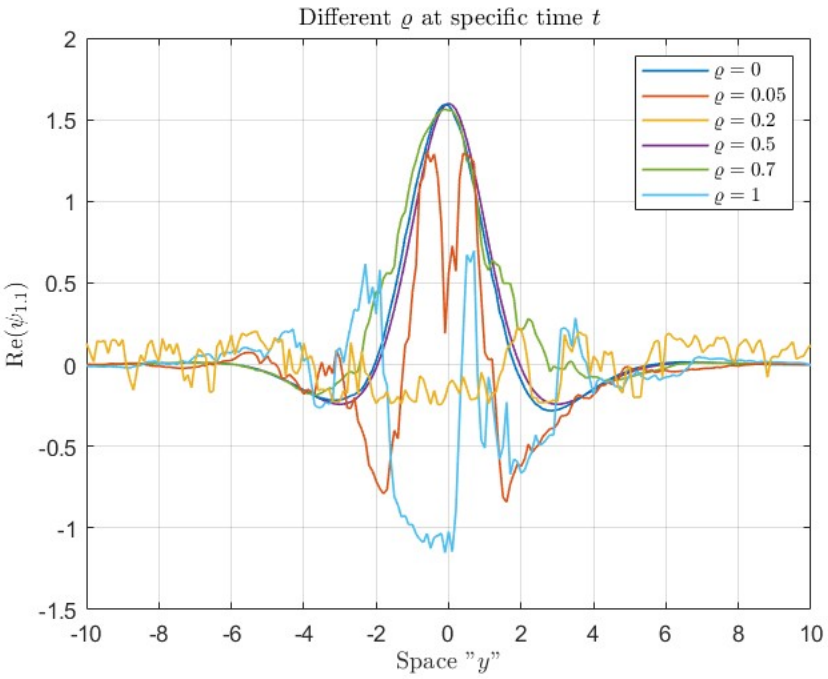

FIGURE 4. Collective two-dimensional plot the real part of Eq. (3.7) along the $y-$direction with different noise intensities.

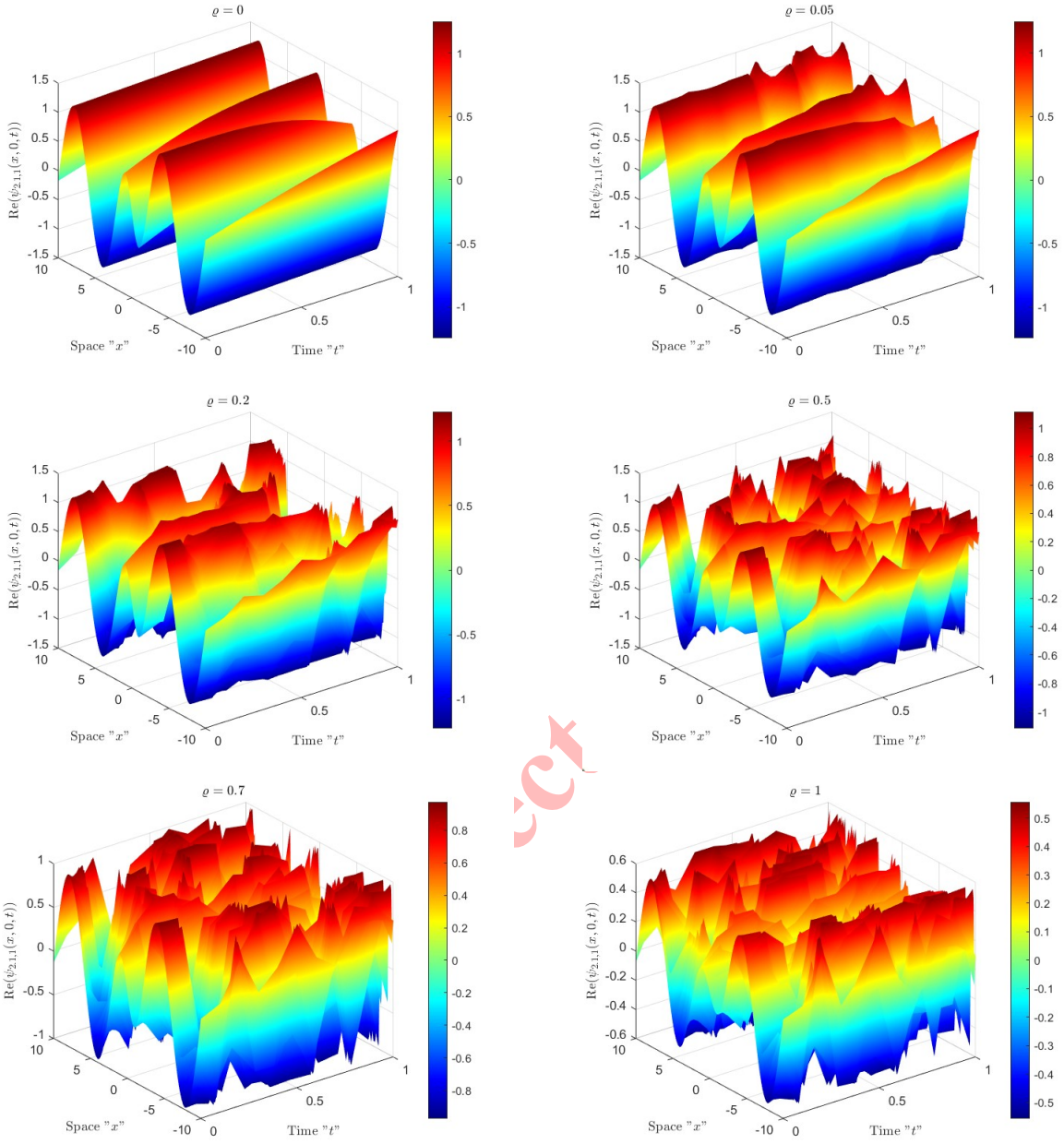

FIGURE 5. Three-dimensional plots of the real part of Eq. (3.10) along the $x-$direction with different noise intensities.

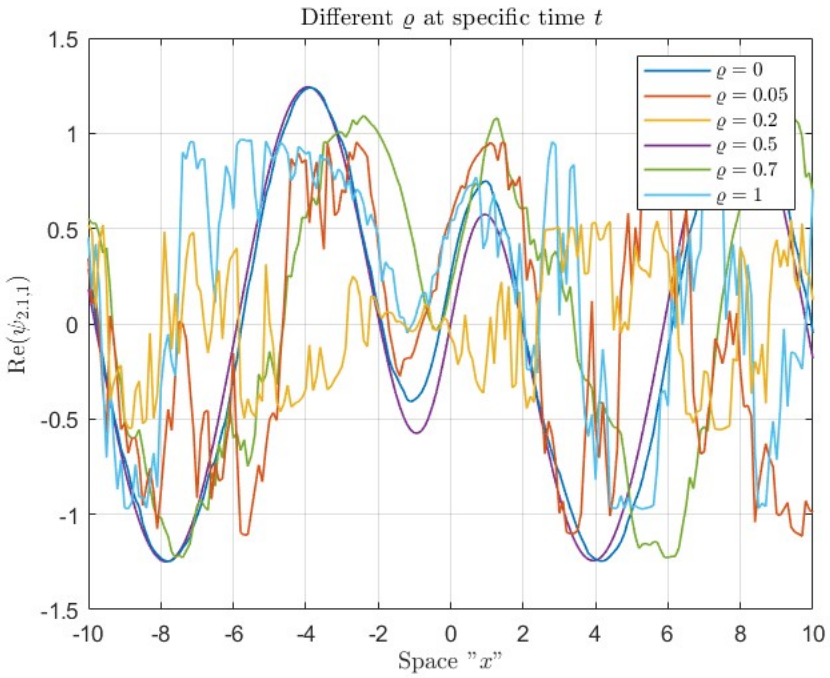

FIGURE 6. Collective two-dimensional plot the real part of Eq. (3.10) along the $x-$direction with different noise intensities.

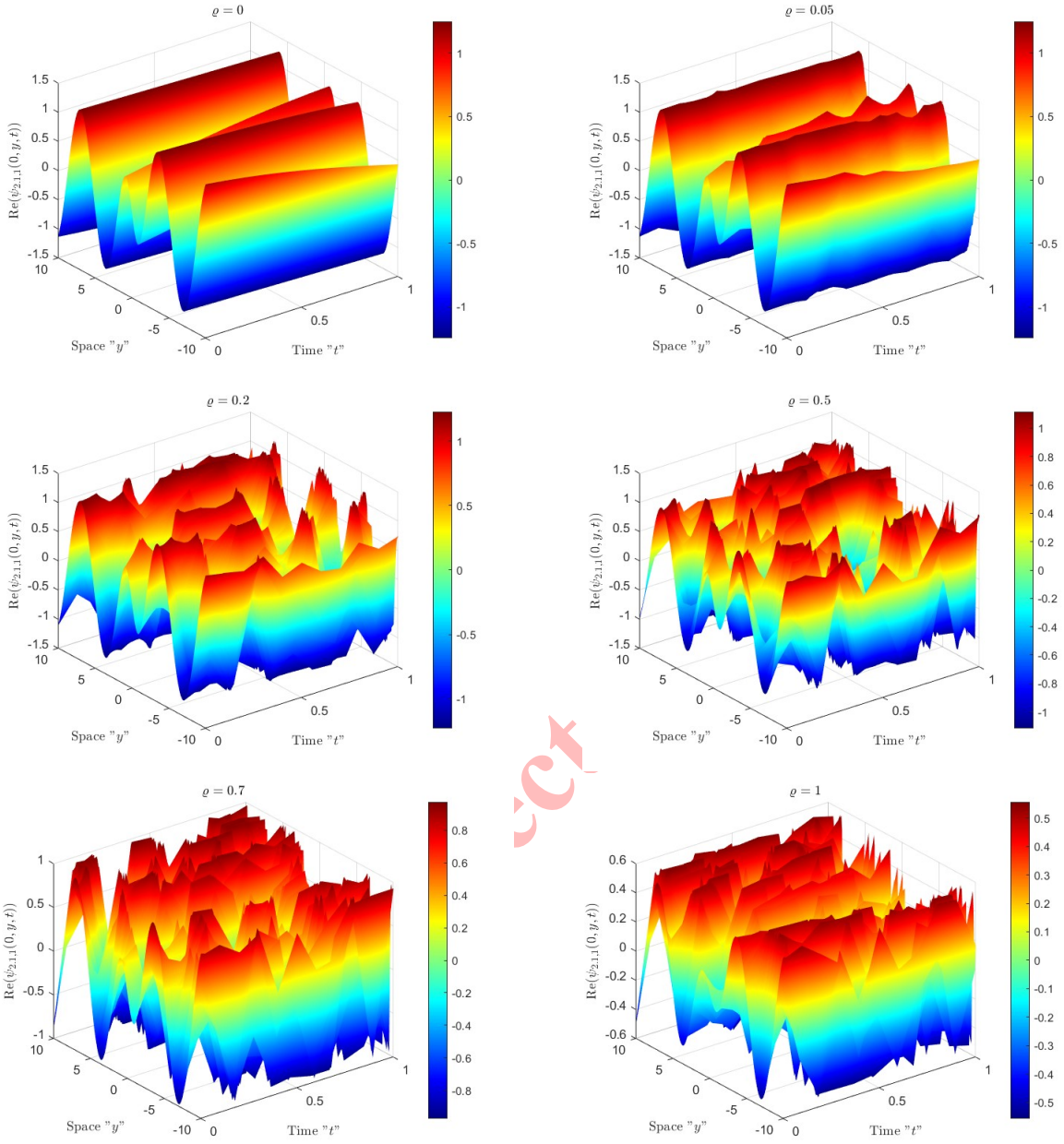

FIGURE 7. Three-dimensional plots of the real part of Eq. (3.10) along the $y-$direction with different noise intensities.

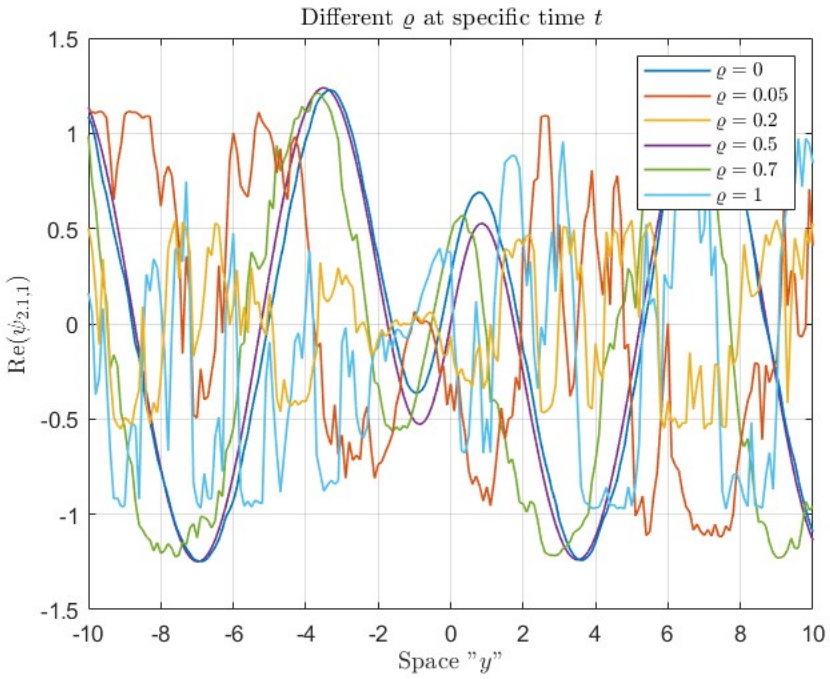

FIGURE 8. Collective two-dimensional plot the real part of Eq. (3.10) along the $y-$direction with different noise intensities.

References

[1] K. K. Ahmed, N. M. Badra, H. M. Ahmed, and W. B. Rabie, *Soliton solutions and other solutions for Kundu–Eckhaus equation with quintic nonlinearity and Raman effect using the improved modified extended tanh function method*, Mathematics, *10* (2022), 4203.

[2] K. K. Ahmed, N. M. Badra, H. M. Ahmed, and W. B. Rabie, *Soliton solutions of generalized Kundu-Eckhaus equation with an extra-dispersion via improved modified extended tanh function technique*, Optical and Quantum Electronics, *55* (2023), 299.

[3] K. K. Ahmed, H. M. Ahmed, N. M. Badra, and W. B. Rabie, *Optical solitons retrieval for an extension of novel dual-mode of a dispersive non-linear Schrödinger equation*, Optik, *307* (2024), 171 835.

[4] K. K. Ahmed, N. M. Badra, H. M. Ahmed, and W. B. Rabie, *Unveiling optical solitons and other solutions for fourth-order (2+ 1)-dimensional nonlinear Schrödinger equation by modified extended direct algebraic method*, Journal of Optics,*1* (2024), 1–13.

[5] K. K. Ahmed, N. M. Badra, H. M. Ahmed, W. B. Rabie, M. Mirzazadeh, M. Eslami, and M. S. Hashemi, *Investigation of solitons in magneto-optic waveguides with Kudryashov's law nonlinear refractive index for coupled system of generalized nonlinear Schrödinger's equations using modified extended mapping method*, Nonlinear Analysis: Modelling and Control, *29* (2024), 205-223.

[6] K. K. Ahmed, H. M. Ahmed, N. M. Badra, M. Mirzazadeh, W. B. Rabie, and M. Eslami, *Diverse exact solutions to Davey–Stewartson model using modified extended mapping method*, Nonlinear Analysis: Modelling and Control, *29* (2024), 983-1002.

[7] K. K. Ahmed, H. M. Ahmed, W. B. Rabie, and M. F. Shehab, *Effect of noise on wave solitons for (3+ 1)-dimensional nonlinear Schrödinger equation in optical fiber*, Indian Journal of Physics, *98* (2024), 4863-4882.

[8] K. K. Ahmed, H. M. Ahmed, M. F. Shehab, T. A. Khalil, H. Emadifar, and W. B. Rabie, *Characterizing stochastic solitons behavior in (3+ 1)-dimensional Schrödinger equation with Cubic-Quintic nonlinearity using improved modified extended tanh function scheme*, Physics Open, *21*(2024), 100233.

[9] M. S. Algolam, A. I. Ahmed, H. M. Alshammary, F. E. Mansour, and W. W. Mohammed, *The impact of standard Wiener process on the optical solutions of the stochastic nonlinear Kodama equation using two different methods*, Journal of Low Frequency Noise, Vibration and Active Control, *43* (2024), 1939-1952.

[10] Y. Alhojilan and H. M. Ahmed, *Novel analytical solutions of stochastic Ginzburg-Landau equation driven by Wiener process via the improved modified extended tanh function method*, Alexandria Engineering Journal, *72* (2023), 269–274.

[11] N. H. Ali, S. A. Mohammed, and J. Manafian, *Study on the simplified mch equation and the combined KdV-mKdV equations with solitary wave solutions*, Partial Differential Equations in Applied Mathematics, *9* (2024), 100 599.

[12] R. Ashraf, F. Amanat, F. Ashraf, S. Owyed, R. T. Matoog, M. Mahmoud, and A. Akgül, *Soliton solutions for the (4+ 1)-dimensional Fokas equation using integration techniques*, Alexandria Engineering Journal, *107* (2024), 61–72.

[13] M. H. Bashar and S. R. Islam,*Exact solutions to the (2+1)-dimensional Heisenberg ferromagnetic spin chain equation by using modified simple equation and improve F-expansion methods*, Physics Open, 5 (2020), 100027.

[14] H. Bulut, T. A. Sulaiman, and H. M. Baskonus, *On the new soliton and optical wave structures to some nonlinear evolution equations*, The European Physical Journal Plus, *132* (2017), 459.

[15] M. Daniel and L. Kavitha, *Magnetization reversal through soliton flip in a biquadratic ferromagnet with varying exchange interactions*, Physics Review, *66* (2002), 184433.

[16] B. Guo, L. Ling, and Q. P. Liu, *Nonlinear Schrödinger equation: generalized Darboux transformation and rogue wave solutions*, Physical Review E,*85* (2012), 026607.

[17] K. Hosseini, S. Salahshour, M. Mirzazadeh, A. Ahmadian, D. Baleanu, and A. Khoshrang, *The (2+1)-dimensional Heisenberg ferromagnetic spin chain equation: its solitons and Jacobi elliptic function solutions*, The European Physical Journal Plus, *136* (2021), 206.

[18] A. S. Khalifa, H. M. Ahmed, N. M. Badra, and W. B. Rabie, *Exploring solitons in optical twin-core couplers with Kerr law of nonlinear refractive index using the modified extended direct algebraic method*, Optical and Quantum Electronics, *56* (2024), 1060.

[19] A. S. Khalifa, H. M. Ahmed, N. M. Badra, W. B. Rabie, F. M. Al-Askar, and W. W. Mohammed, *New soliton wave structure and modulation instability analysis for nonlinear Schrödinger equation with cubic, quintic, septic, and nonic nonlinearities*, AIMS Math., *9* (2024), 26166–26181.

[20] B. Kopçasız and E. Yaşar, *Inquisition of optical soliton structure and qualitative analysis for the complex-coupled Kuralay system*, Modern Physics Letters B, *39* (2025), 2450512.

[21] M. Inc, A. I. Aliyu, A. Yusuf, and D. Baleanu, *Optical solitons and modulation instability analysis of an integrable model of (2+1)-dimensional Heisenberg ferromagnetic spin chain equation*, Superlattices and Microstructures, *112* (2017), 628–638.

[22] H. Kumar, A. Malik, and F. Chand, *Analytical spatiotemporal soliton solutions to (3+1)-dimensional cubic-quintic nonlinear Schrödinger equation with distributed coefficients*, Journal of Mathematical Physics, *53* (2012), 103704.

[23] S. Kumar and N. Mann, *Abundant closed-form solutions of the (3+1)-dimensional Vakhnenko-Parkes equation describing the dynamics of various solitary waves in ocean engineering*, Journal of Ocean Engineering and Science,*17* (2022).

[24] S. Kumar and S. K. Dhiman, *Lie symmetry analysis, optimal system, exact solutions and dynamics of solitons of a (3+1)-dimensional generalised BKP-Boussinesq equation*, Pramana-Journal of Physics, *96* (2022), 31.

[25] M. Latha and C. C. Vasanthi, *An integrable model of (2+1)-dimensional Heisenberg ferromagnetic spin chain and soliton excitations*, Physica Scripta, *6* (2014), 065204.

[26] B. Q. Li and Y. L. Ma, *Characteristics of rogue waves for a (2+1)-dimensional Heisenberg ferromagnetic spin chain system*, Journal of Magnetism and Magnetic Materials, *474*(2019), 537–543.

[27] B. Q. Li and Y. L. Ma, *Characteristics of rogue waves for a (2+1)-dimensional Heisenberg ferromagnetic spin chain system*, J. Magn. Magn. Mater. *474* (2019), 537–543.

[28] Y. H. Liang and K. J. Wang, *Diverse wave solutions to the new extended (2+ 1)-dimensional nonlinear evolution equation: Phase portrait, bifurcation and sensitivity analysis, chaotic pattern, variational principle and Hamiltonian*, International Journal of Geometric Methods in Modern Physics,*1* 2550158 (2025).

[29] J. H. Liu, Y. N. Yang, K. J. Wang, and H. W. Zhu, *On the variational principles of the Burgers-Korteweg-de Vries equation in fluid mechanics*, Europhysics Letters, *149* (2025), 52001.

[30] Y. L. Ma, B. Q. Li, and Y. Y. Fu, *A series of the solutions for the Heisenberg ferromagnetic spin chain equation*, Mathematical Methods in the Applied Sciences, *41*(2018), 3316–3322.

[31] W. W. Mohammed, C. Cesarano, N. I. Alqsair, and R. Sidaoui, *The impact of Brownian motion on the optical solutions of the stochastic ultra-short pulses mathematical model*, Alexandria Engineering Journal, *101* (2024), 186-192.

[32] M. A. S. Murad, *Optical solutions to conformable nonlinear Schrödinger equation with cubic–quintic–septimal in weakly non-local media by new Kudryashov approach*, Mod. Phys. Lett. B. *39* (2024), 2550063.

[33] M. A. S. Murad, *Formation of optical soliton wave profiles of nonlinear conformable Schrödinger equation in weakly non-local media: Kudryashov auxiliary equation method*, J. Opt., *1*(2024), 1-14.

[34] M. S. Osman, K. U. Tariq, A. Bekir, A. Elmoasry, N. S. Elazab, M. Younis, and M. Abdel-Aty, *Investigation of soliton solutions with different wave structures to the (2+1)- dimensional Heisenberg ferromagnetic spin chain equation*, Communications in Theoretical Physics, *72*) (2020), 035002.

[35] W. B. Rabie, K. K. Ahmed, N. M. Badra, H. M. Ahmed, M. Mirzazadeh, and M. Eslami, *New solitons and other exact wave solutions for coupled system of perturbed highly dispersive CGLE in birefringent fibers with polynomial nonlinearity law*, Optical and Quantum Electronics, *56* (2024), 1–22.

[36] H. U. Rehman, A. U. Awan, S. M. Eldin, and I. Iqbal, *Study of optical stochastic solitons of Biswas-Arshed equation with multiplicative noise*, AIMS Math. *8* (2023), 21606—21621.

[37] S. Sahooa, and A. Tripathy, *New exact solitary solutions of the (2+1)-dimensional Heisenberg ferromagnetic spin chain equation*, The European Physical Journal Plus, *137* (2022), 390.

[38] I. Samir, K. K. Ahmed, H. M. Ahmed, H. Emadifar, and W. B. Rabie, *Extraction of newly soliton wave structure of generalized stochastic NLSE with standard Brownian motion, quintuple power law of nonlinearity and nonlinear chromatic dispersion*, Physics Open, *21* (2024), 100232.

[39] K. J. Wang, X. L. Liu, W. D. Wang, S. Li, and H. W. Zhu, *Novel singular and non-singular complexiton, interaction wave and the complex multi-soliton solutions to the generalized nonlinear evolution equation*, Modern Physics Letters B, *39* (2025), 2550135.

[40] K. J. Wang, H. W. Zhu, F. Shi, X. L. Liu, G. D. Wang, and G. Li, *Lump wave, breather wave and other abundant wave solutions to the (2+ 1)-dimensional Sawada–Kotera–Kadomtsev–Petviashvili equation of fluid mechanics*, Pramana, *99* (2025), 1–12.

[41] K. J. Wang, *The generalized (3+ 1)-dimensional B-type Kadomtsev–Petviashvili equation: resonant multiple soliton, N-soliton, soliton molecules and the interaction solutions*, Nonlinear Dynamics, *112* (2024), 7309–7324.

[42] K. J. Wang, *Resonant multiple wave, periodic wave and interaction solutions of the new extended (3+ 1)-dimensional Boiti-Leon-Manna-Pempinelli equation*, Nonlinear Dynamics, *111*) (2023), 16427–16439.

[43] K. J. Wang, B. R. Zou, H. W. Zhu, S. Li, and G. Li, *Phase portrait, bifurcation and chaotic analysis, variational principle, hamiltonian, novel solitary, and periodic wave solutions of the new extended Korteweg–de Vries–Type equation*, Mathematical Methods in the Applied Sciences, *48* (2025), 9901-9909.

[44] K. J. Wang, *A fast insight into the optical solitons of the generalized third-order nonlinear Schrödinger's equation*, Results in Physics, *40* (2022), 105872.

[45] H. Yasmin, A. S. Alshehry, A. H. Ganie, A. Shafee, and R. Shah, *Noise effect on soliton phenomena in fractional stochastic Kraenkel-Manna-Merle system arising in ferromagnetic materials*, Scientific Reports, *14* (2024), 1810.

[46] E. H. Zahran and A. Bekir, *Enormous soliton solutions to a (2+ 1)-dimensional Heisenberg ferromagnetic spin chain equation*, Chinese Journal of Physics, *77* (2022), 1236-1252.

[47] E. M. Zayed, A. G. Al-Nowehy, and M. E. Elshater, *Solitons and other solutions to nonlinear Schrödinger equation with fourth-order dispersion and dual power law nonlinearity using several different techniques*, The European Physical Journal Plus, *132* (2017), 1–4.

[48] D. W. Zuo, Y. T. Gao, L. Xue, and Y. J. Feng, *Lax pair, roguewave and soliton solutions for a variable-coefficient generalized nonlinear Schrödinger equation in an optical fiber, fluid or plasma*, Optical and Quantum Electronics, *48* (2016), 1–4.

[49] Q. Zhu and J. Qi, *Abundant Exact Soliton Solutions of the (2+ 1)-Dimensional Heisenberg Ferromagnetic Spin Chain Equation Based on the Jacobi Elliptic Function Ideas*, Advances in Mathematical Physics, *1* (2022), 7422491.

[50] Q. Zhou, Q. Zhu, and A. Biswas, *Optical solitons in birefringent fibers with parabolic law nonlinearity*, Optica Applicata, *44* (3) (2014), 399–409.

[51] H. Zulfiqar, A. Aashiq, K. U. Tariq, H. Ahmad, B. Almohsen, M. Aslam, and H. U. Rehman, *On the solitonic wave structures and stability analysis of the stochastic nonlinear Schrödinger equation with the impact of multiplicative noise*, Optik, *289* (2023), 171250.